DALTON
FULL PAPER

Theory predicts that the weaker π-accepting ligand diaminoborylene occupies the equatorial position in $(OC)_4Fe–B(NH_2)$: theoretical study of $(OC)_4Fe–B(NH_2)$ and $(OC)_4Fe–BH$ †

Yu Chen and Gernot Frenking *

Fachbereich Chemie, Philipps-Universität Marburg, D-35032 Marburg, Germany

Received 31st July 2000, Accepted 18th December 2000
First published as an Advance Article on the web 26th January 2001

Quantum chemical calculations at the NL-DFT (BP86, B3LYP) and CCSD(T) levels of theory predicted that the borylene ligand in $(OC)_4Fe–B(NH_2)$ occupies the equatorial position, while the axial and equatorial forms of the parent compound $(OC)_4Fe–BH$ are energetically nearly degenerate. The axial isomer $(OC)_4Fe–B(NH_2)$ is a transition state on the potential energy surface. Charge and energy analysis of the bonding situation suggests that the borylene ligands are rather strong π acceptors. The strengths of the Fe→BR (R = NH_2 or H) π-back donation in the axial and equatorial plane are very different from each other which yields very different bond lengths and bond angles of the axial and equatorial CO ligands. The calculations show that $B(NH_2)$ is a weaker π-accepting ligand than BH, which contradicts the qualitative rule that the equatorial position is occupied by the better π acceptor.

Introduction

Transition metal (TM) complexes with Group 13 diyl ligands ER (E = B to Tl) have been the subject of numerous experimental[2] and theoretical[3] investigations in recent years. The first Group 13 diyl complex which could be identified in 1995 by X-ray structural analysis was $(OC)_4Fe–AlCp^*$.[4] The analogous boron complex $(OC)_4Fe–BCp^*$ was also synthesized and measured by X-ray structural analysis.[5] Both complexes $(OC)_4Fe–ECp^*$ (E = B or Al) have the diyl ligand in the axial position. The only other TM borylene complex for which an X-ray structural analysis has been reported is $(OC)_5W–B[N(SiMe_3)_2]$.[6] The iron complex has also been synthesized, but its geometry could not be determined by X-ray structural analysis.[6]

Recently, the structure and bonding situation of TM complexes with the ligands BF, $B(NH_2)$, $B(NMe_2)$, and BO^-, which are isolobal analogues of CO, have been the subject of a theoretical investigation at the non-local DFT level of theory by Ehlers *et al.*[7] The authors reported the equilibrium geometries of the borylene complexes $(OC)_4Fe–BR$ with different substituents R. It was stated that the energetically lowest lying isomers have the BR group in the axial position. The equatorial isomers of all investigated ligands were theoretically predicted to be 2–5 kcal mol^{-1} higher in energy than the axial forms.[7] This result is at variance with our previous study of $(OC)_4Fe–B(NH_2)$ where we reported that the borylene ligand is in the equatorial position.[8] The axial isomer of $(OC)_4Fe–B(NH_2)$ was found by us to be a transition state. A very recent theoretical study by Macdonald and Cowley[9] considered only the axial isomer of $(OC)_4Fe–B(NH_2)$ without calculating the vibrational frequencies of the optimized geometries. This was justified with the paper of Ehlers *et al.*[7] where the axial form was claimed to be lower in energy than the equatorial form.

In this paper we report a reinvestigation of the axial and equatorial forms of $(OC)_4Fe–B(NH_2)$ **1** and the parent system $(OC)_4Fe–BH$ **2** at different levels of theory. The calculations predict that the borylene ligand should occupy the equatorial position in **1**. We also report an analysis of the iron–borylene bonding using charge and energy decomposition methods.

† Theoretical studies of inorganic compounds. Part XIII.[1]

Methods

The geometries have been optimized with GAUSSIAN 98[10] at the B3LYP[11] and BP86[3,11a,12] levels of theory using a small-core ECP (effective core potential)[13] with a (441/2111/41) valence basis set for Fe and 6-31G(d) for the other atoms. This is our standard basis set II.[14] Single-point energy calculations have been performed at the CCSD(T)/II[15] level using the BP86/II optimized geometries. Energy calculations have also been carried out at B3LYP, BP86 and CCSD(T) levels with the basis set combination III. Basis set III has the same ECP[13] as basis set II but a larger valence basis set for Fe (4311/2111/311/1) and 6-311G(d) for the other atoms. The exponent for the f-type polarization function has been taken from the literature.[16] Calculations of the vibrational frequencies have been carried out in order to see if the optimized structures are either minima (number of imaginary frequencies $i = 0$) or transition states ($i = 1$). We also optimised the geometries of the compounds with the program package ADF[17] at the BP86 level using a large uncontracted set of Slater-type orbitals (STOs)[18] which has triple-ζ quality for iron. Triple-ζ basis sets augmented by one set of d-type and one set of f-type polarization functions for boron, nitrogen, carbon, oxygen and one set of p and d functions for hydrogen have been used. This basis set combination is called TZ(2)P. The core electrons were treated by the frozen-core approximation.[19] An auxiliary set of s, p, d, f and g STOs was used to fit the molecular densities and to represent the Coulomb and exchange potentials accurately in each SCF cycle.[20] Relativistic effects have been considered by the zero-order regular approximation (ZORA).[21]

For the investigation of the bonding situation we used the charge decomposition analysis (CDA)[22] and the natural bond orbital (NBO)[23] method. In the former method the molecular orbitals of the complexes are expressed as a linear combination of the MOs of the ligand and the metal fragment. The results can be used as a quantitative expression of the Dewar–Chatt–Duncanson model for donor–acceptor interactions.[24]

We also carried out energy analyses of the Fe–CO and Fe–BR interactions with the help of the energy decomposition scheme ETS developed by Ziegler and Rauk.[25] The bond dissociation energy ΔE between two fragments A and B is first separated into two major components ΔE_{prep} and ΔE_{int},

 DOI: 10.1039/b006180h

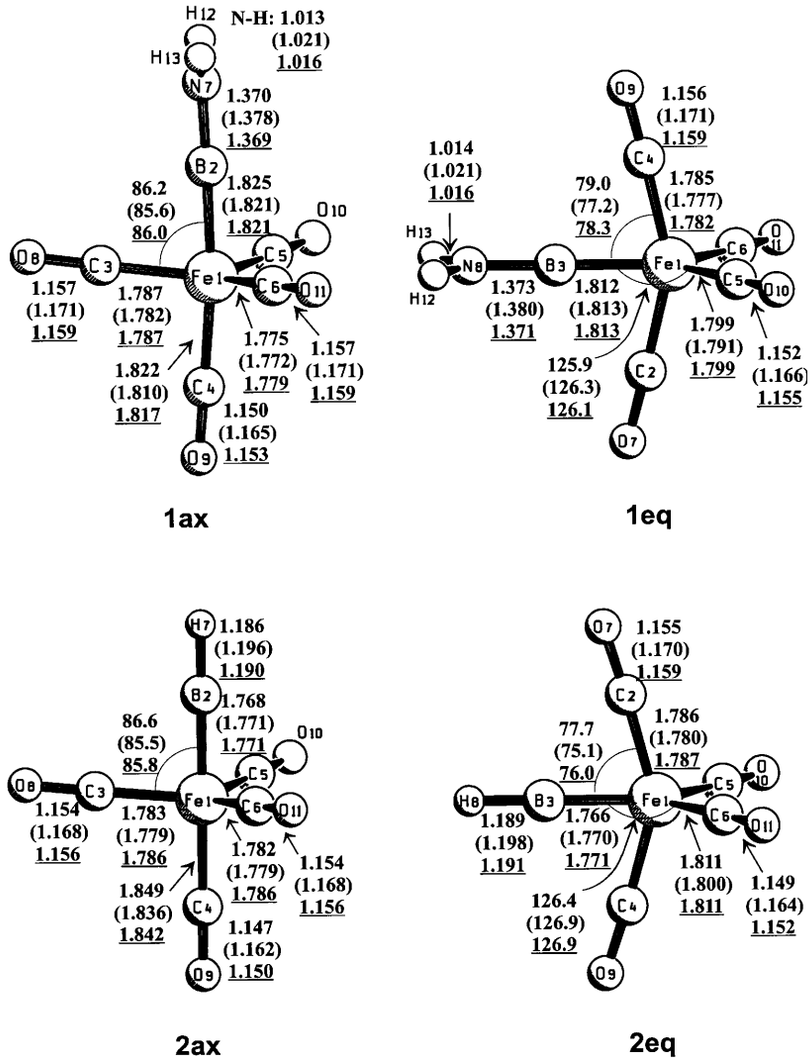

Fig. 1 Optimized geometries of **1ax**, **1eq**, **2ax** and **2eq** at the B3LYP/II (BP86/II) and BP86/TZ(2P) levels. Distances in Å, angles in degrees.

eqn. (1). ΔE_{prep} is the energy which is necessary to promote the

$$\Delta E = \Delta E_{prep} + \Delta E_{int} \quad (1)$$

fragments A and B from their equilibrium geometry and electronic ground state to the geometry and electronic state which they have in the compound AB. ΔE_{int} is the instantaneous interaction energy between the two fragments in the molecule and can be divided into three main components, eqn. (2). ΔE_{elstat}

$$\Delta E_{int} = \Delta E_{elstat} + \Delta E_{Pauli} + \Delta E_{orb} \quad (2)$$

gives the electrostatic interaction energy between the fragments which are calculated with the frozen electron density distribution of A and B in the geometry of the complex AB. The second term ΔE_{Pauli} gives the four-electron destabilizing interactions between occupied orbitals. It is calculated by enforcing the Kohn–Sham determinant of AB, which results from superimposing fragments A and B, to obey the Pauli principle through antisymmetrization and renormalization. The stabilizing orbital interaction term ΔE_{orb} is calculated in the final step of the ETS analysis when the Kohn–Sham orbitals relax to their optimal form. The latter term can be further partitioned into contributions by the orbitals which belong to different irreducible representations of the interacting system.

Geometries and energies

Fig. 1 shows the optimized geometries of the axial (**ax**) and equatorial (**eq**) isomers of the two compounds at the B3LYP and BP86 levels using our standard basis set II.[14] We also optimized the geometries at BP86 using a large uncontracted set of STOs which has TZ(2)P quality.[18] The geometry of **1ax** is similar to that of the previously reported structure.[7] However, the theoretically predicted metal–ligand bond distances Fe–B (1.821–1.825 Å), Fe–CO_{trans} (1.810–1.822 Å) and Fe–CO_{cis} (1.772–1.779 and 1.782–1.787 Å) are ≈0.02 Å shorter than the values which have been reported for **1ax** by Ehlers *et al.*[7] We have no explanation for the discrepancy, because the latter authors used a very similar theoretical level (BP86/TZP) to that we employed in our calculations.

The most interesting feature of the optimized geometries is the tilting of the axial CO groups towards the borylene ligand (Fig. 1). The average angle between the CO_{eq} and $B(NH_2)$ ligands in **1ax** is 86.2° at the B3LYP/II level (85.6° the BP86/II, 86.0° at BP/TZ(2)P). An even stronger umbrella effect is predicted for the equatorial isomer **1eq** (Fig. 1). It is important to recognize that a tilting is only found for the axial CO bonds of **1eq**. The bond angle between CO_{ax} and $B(NH_2)$ is 79.0° at B3LYP/II (77.2° at BP86/II, 78.3° at BP86/TZ(2)P). The equatorial CO ligands are bent away from the borylene ligand. The B–Fe–CO values for the equatorial CO bonds (125.9° at B3LYP/II, 126.3° at BP86/II, 126.1° at BP86/TZ(2)P) suggest that the strengths of the iron–boron π interactions in the axial and equatorial plane are quite different. This aspect will be discussed below in the section on the bonding analysis. It could be argued that the different tilting angles of the axial and equatorial CO ligands in **1eq** are found because of the

Table 1 Calculated relative energies E_{rel} and Fe–B bond dissociation energies D_e and D_o in kcal mol^{-1}

		$(OC)_4Fe–B(NH_2)$		$(OC)_4Fe–BH$	
		1ax	**1eq**	**2ax**	**2eq**
BP86/II	E_{rel}	0.0	−2.1	0.0	0.3
	i	1	0	0	0
	$D_e(D_o)^a$	89.5(85.9)	91.6(87.5)	105.3(100.7)	105.0(100.3)
BP86/II	E_{rel}	0.0	2.0(−1.4)^b	0.0	1.4(1.4)^b
	$D_e(D_o)^a$	85.6(82.0)	83.6(79.5)	103.5(99.0)	102.0(97.3)
BP86/TZ(2)P	E_{rel}	0.0	−1.7	0.0	0.7
	D_e	86.8	88.3	105.3	104.5
B3LYP/II	E_{rel}	0.0	−2.7	0.0	−0.5
	i	1	0	0	0
	$D_e(D_o)^a$	80.3(76.6)	83.0(78.7)	94.8(90.0)	05.3(90.3)
B3LYP/III	E_{rel}	0.0	−2.8(−2.7)^b	0.0	−0.3(−0.3)^b
	$D_e(D_o)^a$	75.3(71.6)	78.0(73.8)	89.2(84.4)	89.6(84.6)
CCSD(T)/II^c	E_{rel}	0.0	−3.3	0.0	−1.1
	$D_e(D_o)^a$	88.8(85.2)	92.1(88.0)	102.3(94.5)	103.3(95.4)
CCSD(T)/III^c	E_{rel}	0.0	−2.8	0.0	0.5
	$D_e(D_o)^a$	85.0(81.4)	87.8(83.7)	101.3(96.8)	100.8(96.1)

^{a} D_o values are calculated by zero-point vibrational energy (ZPE) correction. ^{b} Using a larger grid size = 99590 instead of the default value 75302. ^{c} Using BP86/II optimized geometries and ZPE.

difference between the in-plane and out-of-plane B–(NH_2) π interaction. This is not true. The parent compound **2eq** exhibits an even stronger tilting of the axial but not of the equatorial CO groups towards the borylene ligand BH (Fig. 1). Note that the strongly tilted axial CO groups in **1eq** and particularly in **2eq** have significantly shorter Fe–CO bond lengths than those of the equatorial CO ligands. The axial form **2ax** has similar tilting of the CO ligands to that of **1ax**.

Table 1 shows the calculated energies. The equatorial isomer **1eq** is theoretically predicted at BP86/II, B3LYP/II and CCSD(T)/II//BP86/II levels to be 2.1–3.3 kcal mol^{-1} lower in energy than **1ax**! Calculations of the Hessian matrix with both DFT methods also show that **1ax** is not a minimum on the potential energy surface. The equilibrium structure **1ax** is a transition state which has one negative eigenvalue. The associated imaginary mode does not belong to the rotation of the $B(NH_2)$ group about the B–N axis, but rather to the Berry pseudorotation. In order to predict the energy difference between **1ax** and **1eq** more accurately we carried out single-point energy calculations with the larger basis set III. The energy difference **1ax**–**1eq** at B3LYP and CCSD(T) levels changes only slightly when the larger basis is employed (Table 1). The equatorial isomer is predicted to be 2.8 kcal mol^{-1} (B3LYP/III or CCSD(T)/III) lower in energy than the axial isomer. We were surprised, however, by the energies which are predicted at the BP86 level with the larger basis set. Table 1 shows that BP86/III calculates **1eq** to be 2.0 kcal mol^{-1} *higher* in energy than **1ax**! We checked the calculations and found that the latter result is an artefact of the standard grid size which is used as default in GAUSSIAN 98. We changed the grid size from the default value 75302 to the higher value 99590. Calculations at the BP86/III level with the latter grid size predict that **1eq** is 1.4 kcal mol^{-1} lower in energy than **1ax** which is in agreement with the results of the other methods. We recalculated the energies of the compounds at the B3LYP/III level using the larger grid size (Table 1). The relative energy **1ax**–**1eq** changes only little when the standard grid size (75302) becomes larger (99590).

The energy difference between the axial and equatorial forms of the parent molecule $(OC)_4Fe–BH$ **2ax** and **2eq** is smaller than in the case of **1**. BP86/II and BP86/TZ(2)P predict that **2ax** is 0.3 and 0.7 kcal mol^{-1} more stable than **2eq**, respectively, but B3LYP/II and CCSD(T)/II give slightly lower energies for the equatorial isomer. Unlike **1ax**, the axial isomer **2ax** at BP86/II and B3LYP/II is a minimum on the potential energy surface. Calculations with the larger basis set III change the relative energies in favor of **2ax**. The axial isomer is now predicted at the CCSD(T)/III level to be 0.5 kcal mol^{-1} more stable than the equatorial isomer. Note that the BP86 calculations of **2** do not show such a dramatic reversal of the relative energy of the axial and equatorial isomer when the grid size becomes larger (Table 1). The relative energy of **2ax** and **2eq** at the BP86/III level remains the same when the grid size is changed from 75302 to 99590. This shows that the choice of the grid size can be the source of significant errors in the energy calculations which may not easily be noticed.

Table 1 gives also the theoretically predicted bond dissociation energies D_e and the ZPE corrected D_o values of the $(OC)_4Fe–BR$ bonds of compounds **1** and **2**. The Fe–B bonds are very strong. At the highest level of theory, *i.e.* CCSD(T)/III//BP86/II, the Fe–B bond energy of **1eq** is D_e = 87.8 kcal mol^{-1}. The parent compound **2** has a stronger Fe–B bond than **1**. The calculated value for the most stable isomer at CCSD(T)/III//BP86/II **2ax** is D_e = 101.3 kcal mol^{-1}. We want to point out that the B3LYP and BP86 values for the dissociation energies are not very different from the CCSD(T) values.

Analysis of the bonding situation

We investigated the metal–ligand interactions in the diyl complexes with the help of electronic charge and energy partitioning methods. To this end we first analysed the bonding situation in **1**, **2** and $Fe(OC)_5$ using the CDA[22] and NBO[23] methods in order to address the question of the amount of $(OC)_4Fe←L$ σ donation and $(OC)_4Fe→L$ π-back donation. Table 2 gives the results of the two methods. A pictorial description of the change in the π charge at the $B(NH_2)$ and BH ligands given by the NBO method is shown in Fig. 2.

The difference in the orbital population of the boron p(π) AOs in $B(NH_2)$ between the "free" ligand and compound **1eq** indicates that the in-plane p(π) orbital receives significant electronic charge from the iron atom (0.45 e), but also the charge in the out-of-plane p(π) AO increases from 0.23 to 0.41 e (Fig. 2).[26] Note that in complex **1eq** the in-plane p(π) orbital of boron becomes more highly populated than the out-of-plane p(π) AO. The total $(OC)_4Fe→B(NH_2)$ π-back donation in **1eq** given by the NBO method is 0.58 e (Table 2). The largest part (0.45 e) comes from the π donation in the equatorial plane, while the lesser part (0.13 e) comes from the axial π-back donation. Since the total charge of the $B(NH_2)$ ligand is +0.31 e it follows that

Table 2 Results of the CDA and NBO analysis of complexes $Fe(CO)_4L$ (L = BH, $B(NH_2)$ or CO) at the BP86/II level

		CDA			NBO				
$(OC)_4Fe–L$		d^a	b^b	$b:d$	q(L)	p_π(L)	Δq_σ(L)^c	Δq_π(L)^d	$b:d^e$
$(OC)_4Fe–B(NH_2)$(ax)	**1ax**	0.629	0.428	0.68	0.41	0.82[f]	0.94	−0.53	0.56
$(OC)_4Fe–B(NH_2)$(eq)	**1eq**	0.607	0.486	0.80	0.31	0.88[f]	0.89	−0.58	0.65
$(OC)_4Fe–BH$(ax)	**2ax**	0.558	0.549	0.98	0.33	0.67	1.00	−0.67	0.67
$(OC)_4Fe–BH$(eq)	**2eq**	0.532	0.617	1.16	0.21	0.77	0.98	−0.77	0.79
$(OC)_4Fe–CO$(ax)		0.517	0.316	0.61	0.15	4.40	0.55	−0.40	0.73
$(OC)_4Fe–CO$(eq)		0.473	0.307	0.65	0.08	4.36	0.44	−0.36	0.82

[a] L→$Fe(CO)_4$ σ donation. [b] L←$Fe(CO)_4$ π-back donation. [c] Difference between q(L) and Δq_π(L). [d] Difference between the ligand p_π charge in the complex and the "free" ligand. [e] Given by $|\Delta q_\pi(L)|/|\Delta q_\sigma(L)|$. [f] p_π Charge at boron only.

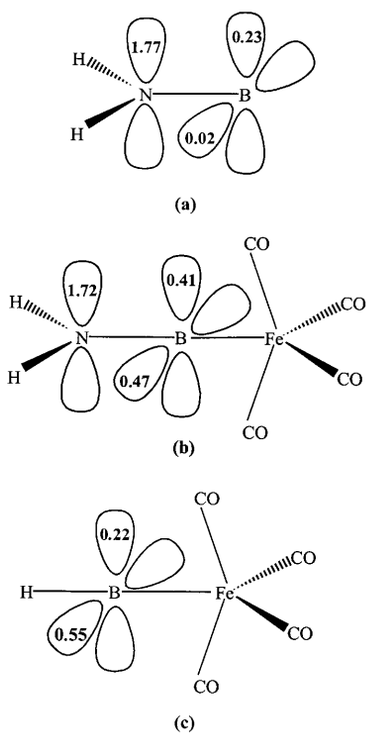

Fig. 2 Calculated NBO population of the p_π ligand orbitals of (a) free $B(NH_2)$; (b) **1eq**; (c) **2eq**.

the $(OC)_4Fe←B(NH_2)$ σ donation is 0.89 e. Even stronger back donation than for $B(NH_2)$ is calculated for the ligand BH. Table 2 shows that the $(OC)_4Fe→BH$ π-back donation in **2eq** is 0.77 e. The equatorial π donation (0.55 e) is like in **1eq** much stronger than the axial π donation (0.22 e) The calculated $(OC)_4Fe←BH$ σ donation is 0.98 e. Thus, the NBO method suggests that $B(NH_2)$ and BH are strong π-accepting ligands but even stronger σ donors.

The CDA also suggests that the borylene groups are rather strong π-acceptor ligands in compound **1** and **2**. This becomes obvious from the ratio of the calculated π-back donation and σ donation ($b:d$) which is given in Table 2. According to the CDA the complex **2eq** even has more back donation than donation. The NBO and CDA results indicate that BH is a stronger π acceptor than $B(NH_2)$. The two methods disagree about the relative acceptor strength of the borylene ligands and CO. The CDA data suggest that $B(NH_2)$ and BH are stronger π-acceptor ligands than CO, while the ratio of the π-back donation and σ donation given by the NBO method ($|\Delta q_\pi|:|\Delta q_\sigma|$) indicates slightly more back donation for CO than for $B(NH_2)$ and BH. It should be noted that the amount of σ and π *charge* transfer does not necessarily correlate with the associated orbital interaction *energies*. The latter are also influenced by the eigenvalues of the interacting orbitals. In order to analyse the energy contributions of the σ and π interactions we carried out ETS analyses of the axial and equatorial isomers of **1** and **2**. A recent systematic study of the bonding situation in 50 transition metal complexes with terminal Group 13 diyl ligands $(OC)_4Fe–ER$, $Fe(EMe)_5$ and $Ni(EMe)_4$ (E = B to Tl; R = Cp, $N(SiH_3)_2$, Ph or Me) showed that the ETS results are very helpful for interpretation of the metal–ligand bonds.[1] The ETS results of **1** and **2** are shown in Table 3.

The data in Table 3 give a detailed insight into the nature of the metal–ligand interactions of compounds **1** and **2**. The Fe–borylene interaction energies ΔE_{int} are significantly higher than the Fe–CO values by a factor of ≈2. Note that the covalent contributions to the bonding interactions given by the percentage of the ΔE_{orb} term of the total attractive terms are not very different between the Fe–BR and Fe–CO bonds. The latter have only a slightly lower ionic character than the former bonds. The ETS results suggest that both metal–ligand bonds are a bit more ionic than covalent.

A pivotal question concerns the strength of the π contributions to the metal–ligand orbital interactions. A qualitative analysis of the orbital interactions in trigonal bipyramidal complexes of d^8 elements led to the conclusion that good π-accepting ligands will prefer the equatorial site.[27] This model is widely used in chemistry textbooks to explain the site preference in the complexes.[28] Table 3 shows that the absolute values of ΔE_π for the Fe–CO bonds are similar (**1ax**) or lower than the data for the Fe–BR bonds. However, the relative contribution of the π-orbital interactions to ΔE_{orb} is much higher for the iron–carbonyl bonds than for the Fe–BR bonds. The Fe–CO bonds have between 47.0 and 55.8% π-orbital contributions while the Fe–BR bonds have only 32.8–39.3% π contributions. The calculated value of 32.8% for the π-orbital contribution of the Fe–B bond in **1ax** is in good agreement with the previous result of 31.0% reported by Ehlers *et al.*[7] The absolute and relative values of the π-orbital contributions agree that the ligand BH is clearly a better π acceptor than is $B(NH_2)$ (Table 3). The above rule suggests that $(OC)_4Fe–BH$ should exhibit a larger preference for the equatorial isomer than $(OC)_4Fe–B(NH_2)$. The calculated energies of the axial and equatorial forms of **1** and **2** clearly show that this is not the case. The contradiction between the calculated energies and the predicted relative stabilities of the isomeric forms can not be explained with steric arguments, because the ligands are rather small. It seems that the electronic factors which lead to a site preference in trigonal bipyramidal complexes of d^8 elements can not solely be explained with the π-acceptor strength of the ligand. The results of the energy analysis suggest that the interplay of several factors may be responsible for the ligand site. A systematic investigation of $(OC)_4Fe–L$ complexes with different ligands L came to the same conclusion.[29]

The σ and π energy contributions to the total orbital interactions in the equatorial structures **1eq** and **2eq** shall finally be discussed with reference to the NBO and CDA data. The σ contributions arise from orbitals which have a_1 symmetry and the π contributions from orbitals which have b_1 symmetry (axial π interactions) and b_2 symmetry (equatorial π interactions).

Table 3 ETS analysis of the Fe–L bonds (L = $B(NH_2)$, BH or CO) of the complexes $Fe(CO)_4(BNH_2)$ and $Fe(CO)_4(BH)$ at the BP86/TZ(2)P level Energy contributions in kcal mol^{-1}

	$Fe(CO)_4[B(NH_2)]$				$Fe(CO)_4(BH)$			
	1ax (L = $B(NH_2)$)	**1ax** (L = CO_{ax})	**1eq** (L = BNH_2)	**1eq** (L = CO_{eq})	**2ax** (L = BH)	**2ax** (L = CO_{ax})	**2eq** (L = BH)	**2eq** (L = CO_{eq})
Symmetry	$C_s[C_s]$	C_s	C_{2v}	C_s	C_{3v}	C_{3v}	C_{2v}	C_s
ΔE_{int}	−96.5	−51.1	−98.1	−52.3	−116.3	−45.8	−117.5	−49.9
ΔE_{Pauli}	245.2	129.0	285.8	138.8	284.2	122.1	341.8	133.3
ΔE_{elstat}	−201.3	−97.0	−229.7	−105.7	−233.9	−91.8	−269.2	−101.9
ΔE_{orb} [a]	−140.4	−83.1	−154.2	−85.4	−166.7	−76.1	−190.1	−81.3
	(41.1%)	(46.1%)	(40.2%)	(44.7%)	(41.6%)	(45.3%)	(41.4%)	(44.4%)
	−113.4(a′)	−59.9(a′)	−99.5(a_1)	−65.0(a′)	−104.1(a_1)	−36.7(a_1)	−115.2(a_1)	−62.2(a′)
	−27.0[−19.0] [b](a″)	−23.2(a″)	−0.3(a_2)	−20.4(a″)	0.0(a_2)	0.0(a_2)	−0.5(a_2)	−19.1(a″)
			−16.5(b_1)		−62.5(e)	−39.4(e)	−26.4(b_1)	
			−37.8(b_2)				−48.1(b_2)	
ΔE_{σ}	−94.4	−36.7	−99.5	−44.6	−104.1	−36.7	−115.2	−43.1
ΔE_{π} [c]	−46.0	−46.4 [d]	−54.3	−40.8 [d]	−62.5	−39.4	−74.5	−38.2 [d]
	(32.8%)	(55.8%)	(35.2%)	(47.8%)	(37.5%)	(51.8%)	(39.3%)	(47.0%)
ΔE_{prep}	9.7	—	9.8	—	11.0	—	13.0	—
$\Delta E = (-D_e)$	−86.8	—	−88.3	—	−105.3	—	−104.5	—

[a] The value in parentheses gives the percentage contribution to the total attractive interactions: $E_{orb}/(E_{orb} + E_{elstat})$. [b] The second value was obtained from a calculation where the NH_2 was rotated by 90° along the B–N axis. [c] The value in parentheses gives the percentage contribution to the total orbital interactions: E_{π}/E_{orb}. [d] The total π interaction was estimated by taking the a″ contribution twice.

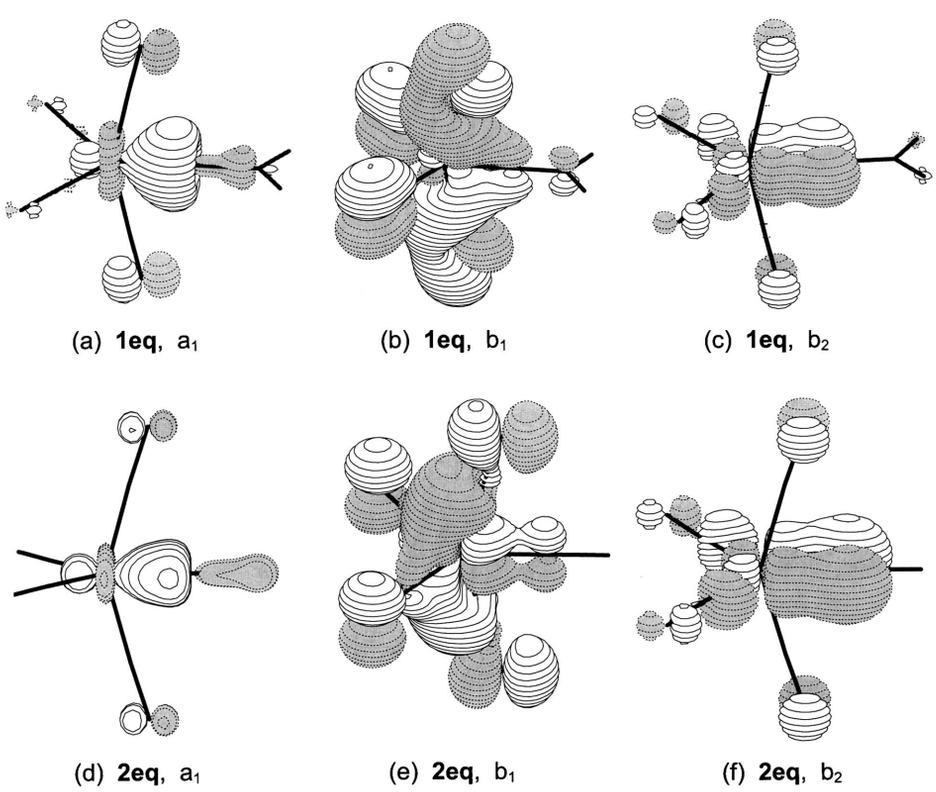

Fig. 3 Contour line diagrams of molecular orbitals calculated at the B3LYP/II level which are relevant for the Fe–BR interactions. (a) HOMO-5 (a_1) of compound **1eq** showing the $(OC)_4Fe \leftarrow B(NH_2)$ σ donation; (b) HOMO-6 (b_1) of **1eq** showing the $(OC)_4Fe \rightarrow B(NH_2)$ π-back donation in the axial plane; (c) HOMO-1 (b_2) of **1eq** showing the $(OC)_4Fe \rightarrow B(NH_2)$ π-back donation in the equatorial plane; (d) HOMO-4 (a_1) of **2eq** showing the $(OC)_4Fe \leftarrow BH$ σ donation; (e) HOMO-3 (b_1) of **2eq** showing the $(OC)_4Fe \rightarrow BH$ π-back donation in the axial plane; (f) HOMO-1 (b_2) of **2eq** showing the $(OC)_4Fe \rightarrow BH$ π-back donation in the equatorial plane.

Fig. 3 shows plots of the relevant orbitals which nicely reflect the orbital interactions. Fig. 3(a) depicts the a_1 orbital which contributes the major part of the σ interactions in $(CO)_4Fe$–$B(NH_2)$ (**1eq**). Fig. 3(b) and 3(c) show the b_1 and b_2 orbitals which give a pictorial description of the equatorial and axial π interactions in the compound. It becomes obvious that the b_2 orbital has much larger Fe–B bonding coefficients than the b_1 orbital, which extends to a large degree in a bonding fashion to the axial Fe–CO bonds. The shapes of the orbitals clearly show that the equatorial (b_2) orbital contributes more to the Fe–B bonding than does the axial (b_1) MO. This is consistent with the calculated energy contributions given by the ETS method (Table 3). The relative energy contributions of the π and σ orbital interactions $\pi(b_1 + b_2) : \sigma(a_1) = 0.55$ agree nicely with the calculated $b:d$ ratio given by the NBO method (0.65) and also with the CDA results (0.80, Table 2) but the latter seems to overestimate the π contributions. Similar results are found for $(CO)_4Fe$–BH **2eq**. Fig. 3(d) depicts a contour line

diagram of the a_1 orbital of **2eq**. The axial and equatorial π interactions are visualized by the b_1 orbital and the b_2 orbitals which are shown in Figs. 3(e) and 3(f). The shapes of the latter orbitals agree nicely with the larger energy contribution of the b_2 orbital interactions than the b_1 interactions. The ratio of the π and σ contributions to the ΔE_{orb} term $\pi(b_1 + b_2):\sigma(a_1) = 0.65$ is in good agreement with the calculated $b:d$ ratio given by the NBO method (0.79) while the CDA results (1.16) wrongly predict that the π contributions are larger than the σ contributions.

The large differences between the Fe→BR (R = NH_2 or H) π-back donation in the axial and equatorial planes in compounds **1eq** and **2eq** explain nicely the calculated equilibrium geometries of the complexes. The stronger π-back donation in the equatorial plane yields less Fe→CO_{eq} π-back donation which makes the Fe–CO_{eq} bonds to become longer than the axial Fe–CO bonds (Fig. 1). The strong tilting of the axial CO ligands towards the borylene ligand and the bending of the equatorial CO ligands away from the BR group are also the result of the different Fe→BR π-back donation.

Conclusion

The results of this paper can be summarized as follows. The energy calculations at different levels of theory give evidence that the ligand $B(NH_2)$ occupies the equatorial position in the complex $(OC)_4Fe–B(NH_2)$. The calculations predict that the borylene ligand of the complex $(OC)_4Fe–B[N(SiMe_3)_2]$ which was synthesized by Braunschweig *et al.*[6] is at the equatorial position. The bulky $B[N(SiMe_3)_2]$ group should even more prefer the less crowded equatorial site. The axial and equatorial forms of $(OC)_4Fe–BH$ are energetically nearly degenerate and it is difficult to predict whether **2ax** or **2eq** is lower in energy. The electronic charge analysis using the CDA and NBO methods indicates that the borylene ligands are rather strong π-accepting ligands. The energy analysis of the Fe–BR bond also indicates that the π orbital interactions are quite strong. However, σ orbital interactions contribute more than the π orbital interactions to the covalent bonding in $(OC)_4Fe–B(NH_2)$ and $(OC)_4Fe–BH$. The Fe–BR bonds in the axial and equatorial forms of **1** and **2** have ≈60% ionic character and ≈40% covalent character. All methods agree that BH is a stronger π accepting ligand than $B(NH_2)$. The stronger preference for the equatorial position of the borylene ligand in $(OC)_4Fe–B(NH_2)$ than in $(OC)_4Fe–BH$ contradicts the model that good π-accepting ligands will prefer the equatorial site. The strengths of the Fe→BR (R = NH_2 or H) π-back donation in the axial and equatorial plane are very different from each other which yields very different bond lengths and bond angles of the axial and equatorial CO ligands.

Acknowledgements

This work was supported by the Deutsche Forschungsgemeinschaft and the Fonds der Chemischen Industrie. Excellent service by the Hochschulrechenzentrum of the Philipps-Universität Marburg is gratefully acknowledged. Additional computer time was provided by the HLRZ Stuttgart and the HHLRZ Darmstadt.

References

1 Part XII, J. Uddin and G. Frenking, *J. Am. Chem. Soc.*, in press.
2 Reviews: H. Braunschweig, *Angew. Chem.*, 1998, **110**, 1882; H. Braunschweig, *Angew. Chem., Int. Ed.*, 1998, **37**, 1786; H. Braunschweig, *Angew. Chem.*, 1999, **111**, 817; B. Wrackmeyer, *Angew. Chem., Int. Ed.*, 1999, **38**, 771; R. A. Fischer and J. Weiß, *Angew. Chem.*, 1999, **111**, 3002; R. A. Fischer and J. Weiß, *Angew. Chem., Int. Ed.*, 1999, **38**, 2830.
3 Review: C. Boehme, J. Uddin and G. Frenking, *Coord. Chem. Rev.*, 2000, **197**, 249.
4 J. Weiß, D. Stetzkamp, B. Nuber, R. A. Fischer, C. Boehme and G. Frenking, *Angew. Chem.*, 1997, **109**, 95; J. Weiß, D. Stetzkamp, B. Nuber, R. A. Fischer, C. Boehme and G. Frenking, *Angew. Chem., Int. Ed. Engl.*, 1997, **36**, 70.
5 A. H. Cowley, V. Lomeli and A. Voigt, *J. Am. Chem. Soc.*, 1998, **120**, 6401.
6 H. Braunschweig, C. Kollann and U. Englert, *Angew. Chem.*, 1998, **110**, 3355; H. Braunschweig, C. Kollann and U. Englert, *Angew. Chem., Int. Ed.*, 1998, **37**, 3179.
7 A. W. Ehlers, E. J. Baerends, F. M. Bickelhaupt and U. Radius, *Chem. Eur. J.*, 1998, **4**, 210. See also F. M. Bickelhaupt, U. Radius, A. W. Ehlers, R. Hoffmann and E. J. Baerends, *New J. Chem.*, 1998, 1.
8 J. Uddin, C. Boehme and G. Frenking, *Organometallics*, 2000, **19**, 571.
9 C. L. B. Macdonald and A. H. Cowley, *J. Am. Chem. Soc.*, 1999, **121**, 12113.
10 GAUSSIAN 98 (Revision A.1), M. J. Frisch, G. W. Trucks, H. B. Schlegel, G. E. Scuseria, M. A. Robb, J. R. Cheeseman, V. G. Zakrzewski, J. A. Montgomery, R. E. Stratmann, J. C. Burant, S. Dapprich. J. M. Milliam, A. D. Daniels, K. N. Kudin, M. C. Strain, O. Farkas, J. Tomasi, V. Barone, M. Cossi, R. Cammi, B. Mennucci, C. Pomelli, C. Adamo, S. Clifford, J. Ochterski, G. A. Petersson, P. Y. Ayala, Q. Cui, K. Morokuma, D. K. Malick, A. D. Rabuck, K. Raghavachari, J. B. Foresman, J. Cioslowski, J. V. Ortiz, B. B. Stefanov, G. Liu, A. Liashenko, P. Piskorz, I. Komaromi, R. Gomberts, R. L. Martin, D. J. Fox, T. A. Keith, M. A. Al-Laham, C. Y. Peng, A. Nanayakkara, C. Gonzalez, M. Challacombe, P. M. W. Gill, B. G. Johnson, W. Chen, M. W. Wong, J. L. Andres, M. Head-Gordon, E. S. Replogle and J. A. Pople, Gaussian Inc., Pittsburgh, PA, 1998.
11 (*a*) A. D. Becke, *Phys. Rev. A*, 1988, **38**, 3098; (*b*) C. Lee, W. Yang and R. G. Parr, *Phys. Rev. B*, 1988, **37**, 785; (*c*) A. D. Becke, *J. Chem. Phys.*, 1993, **98**, 5648; (*d*) P. J. Stevens, F. J. Devlin, C. F. Chablowski and M. J. Frisch, *J. Phys. Chem.*, 1994, **98**, 11623.
12 J. P. Perdew, *Phys. Rev. B*, 1986, **33**, 8822.
13 P. J. Hay and W. R. Wadt, *J. Chem. Phys.*, 1985, **82**, 299.
14 G. Frenking, I. Antes, M. Boehme, S. Dapprich, A. W. Ehlers, V. Jonas, A. Neuhaus, M. Otto, R. Stegmann, A. Veldkamp and S. F. Vyboishchikov, *Reviews in Computational Chemistry*, eds. K. B. Lipkowitz and D. B. Boyd, VCH, New York, 1996, vol. 8, pp. 63–144.
15 J. Cizek, *J. Chem. Phys.*, 1966, **45**, 4256; J. A. Pople, R. Krishnan, H. B. Schlegel and J. S. Binkley, *Int. J. Quantum Chem.*, 1978, **14**, 545; R. J. Bartlett and G. D. Purvis, *Int. J. Quantum Chem.*, 1978, **14**, 561; G. D. Purvis and R. J. Bartlett, *J. Chem. Phys.*, 1982, **76**, 1910; K. Raghavachari, G. W. Trucks, J. A. Pople and M. Head-Gordon, *Chem. Phys. Lett.*, 1989, **157**, 479; R. J. Bartlett, J. D. Watts and S. A. Kucharski, J. Noga, *Chem. Phys. Lett.*, 1990, **165**, 513.
16 A. W. Ehlers, M. Böhme, S. Dapprich, A. Gobbi, A. Höllwarth, V. Jonas, K. F. Köhler, R. Stegmann, A. Veldkamp and G. Frenking, *Chem. Phys. Lett.*, 1993, **208**, 111.
17 ADF99: E. J. Baerends, D. E. Ellis and P. Ros, *Chem. Phys.*, 1973, **2**, 41; L. Versluis and T. Ziegler, *J. Chem. Phys.*, 1988, **322**, 88; G. te Velde and E. J. Baerends, *J. Comput. Phys.*, 1992, **99**, 84; C. Fonseca Guerra, J. G. Snijders, G. te Velde and E. J. Baerends, *Theor. Chim. Acta*, 1998, **99**, 391.
18 J. G. Snijders, E. J. Baerends and P. Vernooijs, *At. Data Nucl. Data Tables*, 1982, **26**, 483.
19 E. J. Baerends, D. E. Ellis and P. Ros, *Chem. Phys.*, 1973, **2**, 41.
20 J. Krijn and E. J. Baerends, *Fit Functions in the HFS-Method*, Internal Report (in dutch), Vrije Universiteit Amsterdam, 1984.
21 C. Chang, M. Pelissier and Ph. Durand, *Phys. Scr.*, 1986, **34**, 394; J.-L. Heully, I. Lindgren, E. Lindroth, S. Lundquist and A.-M. Martensson-Pendrill, *J. Phys. B*, 1986, **19**, 2799; E. van Lenthe, E. J. Baerends and J. G. Snijders, *J. Chem. Phys.*, 1993, **99**, 4597; E. van Lenthe, E. J. Baerends and J. G. Snijders, *J. Chem. Phys.*, 1996, **105**, 6505; E. van Lenthe, R. van Leeuwen, E. J. Baerends and J. G. Snijders, *Int. J. Quantum Chem.*, 1996, **57**, 281.
22 S. Dapprich and G. Frenking, *J. Phys. Chem.*, 1995, **99**, 9352.
23 A. E. Reed, L. A. Curtiss and F. Weinhold, *Chem. Rev.*, 1988, **88**, 899.
24 S. F. Vyboishchikov and G. Frenking, *Chem. Eur. J.*, 1998, **4**, 1439; G. Frenking and U. Pidun, *J. Chem. Soc., Dalton Trans.*, 1997, 1653; U. Pidun and G. Frenking, *J. Organomet. Chem.*, 1996, **525**, 269; U. Pidun and G. Frenking, *Organometallics*, 1995, **14**, 5325; S. F. Vyboishchikov and G. Frenking, *Chem. Eur. J.*, 1998, **4**, 1428; A. W. Ehlers, S. Dapprich, S. F. Vyboishchikov and G. Frenking, *Organometallics*, 1996, **15**, 105; S. Dapprich and G. Frenking, *Organometallics*, 1996, **15**, 4547; G. Frenking, S. Dapprich, K. F. Köhler, W. Koch and J. R. Collins, *Mol. Phys.*, 1996, **89**, 1245;

S. Dapprich and G. Frenking, *Angew. Chem.*, 1995, **107**, 383; S. Dapprich and G. Frenking, *Angew. Chem., Int. Ed. Engl.*, 1995, **34**, 354; S. Fau and G. Frenking, *Mol. Phys.*, 1999, **96**, 519.
25 T. Ziegler and A. Rauk, *Theor. Chim. Acta*, 1977, **46**, 1; T. Ziegler and A. Rauk, *Inorg. Chem.*, 1979, **18**, 1558; T. Ziegler and A. Rauk, *Inorg. Chem.*, 1979, **18**, 1755.
26 Note that the population of the nitrogen p_π orbital in $(OC)_4Fe–B(NH_2)$ is slightly less than in free $B(NH_2)$, which means that the $N\rightarrow B$ π donation in the bonded ligand is a little stronger than in the "free" ligand $B(NH_2)$. This can be explained with the higher electronegativity of the $Fe(CO)_4$ fragment than $B(NH_2)$ (see the calculated charge at the ligand) which makes the boron atom become a stronger π acceptor in the complex than in the "free" ligand.
27 A. R. Rossi and R. Hoffmann, *Inorg. Chem.*, 1975, **14**, 365.
28 J. E. Huheey, E. A. Keiter and R. L. Keiter, *Inorganic Chemistry: Principles of Structure and Reactivity*, 4th edn, Harper Collins College Publishers, New York, 1993 p. 483f; T. A. Albright, J. K. Burdett and M. H. Whangbo, *Orbital Interactions in Chemistry*, Wiley, New York, 1985, p. 325.
29 Y. Chen, M. Hartmann and G. Frenking, *Z. Anorg. Allg. Chem.*, submitted for publication.